

MODELING TECHNIQUES OF THIN-WALLED BEAMS
WITH OPEN CROSS SECTIONS

By Knut S. Skattum
Research Laboratories
General Motors Corporation
Warren, Michigan

ABSTRACT

Warping constraints of thin-walled beams of open cross sections may significantly add to the torsional rigidity of the beams. This property is not included in the conventional beam element available in NASTRAN and makes it impossible to model such beams properly.

This paper presents a composite element which includes the effects of warping and offset shear centers. It is shown to be mathematically consistent with thin-walled open beam theory and can easily be incorporated into any structural analysis program by use of NASTRAN'S standard elements.

A numerical example analyzing the vibration of a channel beam is presented, and, by using the composite element, the numerical results agreed very well with theoretical data.

INTRODUCTION

Thin-walled beams of open cross sections are commonly used in automotive and aircraft structures where it is imperative to insure maximum flexural efficiency without violating practical fabrication and assembly requirements. It turns out that for many cases the static and dynamic response of these structures depends strongly upon the warping constraints of the members. Consequently, proper modeling techniques are essential to insure good numerical results.

The most general beam element available in the present version of NASTRAN (level 12) is based upon the well-known Timoshenko beam theory. This theory, however, neglects warping displacements and assumes that the elastic and centroidal axes coincide. Both these conditions are usually too restrictive when thin-walled open beams are modeled.

Several books and articles have been published treating the theory and applications of thin-walled beams of open cross sections. A thorough presentation is found in Vlasov's book (Ref. 1). Timoshenko and Gere have done a

buckling analysis (Ref. 2), and contributions to the vibrational analysis are due to Timoshenko (Ref. 3), Gere (Ref. 4), Gere and Lin (Ref. 5), and Christiano and Salmela (Ref. 6).

This paper presents a new element which includes the effects of warping and noncoincidental elastic and centroidal axes. It is a composite element derived from a variational principle consistent with the thin-walled open beam formulation. Also, in addition to being mathematically correct, this model can very easily be incorporated into any structural analysis program by using elements now available in NASTRAN.

As a numerical example on how the model is constructed, the vibration of a channel beam is analyzed, and good agreement between theoretical and numerical results are obtained.

THEORY OF THIN-WALLED OPEN BEAMS

A thin-walled beam is usually defined by restricting its dimensions so that

$$L > 10d \quad (1)$$

$$d > 10t \quad (2)$$

where L is the length of the bar, d the depth of the cross section, and t the largest thickness (Fig. 1). The first relation makes it possible to assume uniformity of the longitudinal stresses along the axis (St. Venant's Principle) while Eq. 2 is used in making assumptions on the shear stresses in the section. Particularly for beams of open cross sections which will be considered in this analysis, it will be assumed that the middle surface is free of shear. In addition, the material and sectional properties of the beam are assumed to be constant along the length, and the displacements are considered to be small such that the cross sections do not change shapes during deformation.

Figure 1 shows a general thin-walled open beam. Included is also a detail of the cross section giving the locations of the center of gravity (CG) and the shear center (SC). The shear center is the point on the cross section through which the resultant of the transverse shearing forces always passes. Locus of the shear centers along a beam is called the elastic axis, and similarly, the centroidal axis passes through the CG of the cross sections.

Before the differential equations can be presented, it is very important to clearly define the coordinate and displacement system used. Referring to Fig. 1, the x -coordinate coincides with the centroidal axis of the beam, and the y - and z -coordinates are the principal axes of the cross section. The displacements are defined by

u = longitudinal displacement of centroid
 v = vertical displacement of shear center

w = horizontal displacement of shear center
 θ = rotational displacement of shear center

and are also indicated in the figure.

Based on these definitions and the assumptions mentioned above, the full set of differential equations for a thin-walled open beam can be written as (Ref. 1)

$$EA \frac{d^2 u}{dx^2} = -q_x \quad (3)$$

$$EI_1 \frac{d^4 v}{dx^4} = q_y \quad (4)$$

$$EI_2 \frac{d^4 w}{dx^4} = q_z \quad (5)$$

$$EC_\omega \frac{d^4 \theta}{dx^4} - GJ \frac{d^2 \theta}{dx^2} = m_\theta \quad (6)$$

in which E = modulus of elasticity; G = shear modulus; A = cross sectional area; I_1 = moment of inertia about z axis; I_2 = moment of inertia about y-axis; J = torsion constant; C_ω = warping constant; q_x = longitudinal surface load applied to the centroid; q_y and q_z = transverse loads applied at the shear center; and m_θ = twisting moment about the elastic axis.

It should be observed that the above set of differential equations differs from the regular beam equation by the fact that v, w, and θ (and correspondingly q_y , q_z , and m_θ) are displacements (and forces) relating to the shear center rather than the centroid, and that the term

$$EC_\omega \frac{d^4 \theta}{dx^4}$$

relating to the warping of the cross section, has been added. Also, the four equations are completely uncoupled, a very desirable feature made possible by letting some of the displacements be associated with the shear center.

MODELING OF THIN-WALLED OPEN BEAMS

The conventional beam element available in the NASTRAN computer program is essentially based upon the same assumptions given above, but in addition, two other conditions are made:

1. Plane sections remain plane (i.e., no warping deformations)
2. Centroidal- and elastic-axes coincide.

These two additional restrictions were also pointed out in the last section by looking at the differential equations.

Warping is a phenomenon that occurs in all bars subjected to twist, with the exception of circular cross sections (Ref. 7). Only for open sections though can the strain associated with the warping be large enough to cause significant contribution to the rotational stiffness of the beam. By excluding warping, the rotational stiffness is too flexible; a factor of two or more is quite common depending upon the cross-sectional properties and how the beam rotates. There have been some attempts to incorporate warping in the conventional beam element by defining an effective torsional constant J_e . From Eq. 6 it is observed that this can be accomplished by the equation

$$GJ_e \frac{d\theta}{dx} = GJ \frac{d\theta}{dx} - EC_w \frac{d^3\theta}{dx^3} \quad (7)$$

but it is also noticed that J_e then necessarily must depend upon the solution θ . For static analysis, this approach might be used effectively where the rotational displacement θ can be estimated fairly accurately, but for dynamic analysis, where different modes are extracted in the same analysis, large errors will be introduced.

When centroidal and elastic axes do not coincide, the beam element should be modeled along the elastic axis. Otherwise, it can easily be observed that the bending moment created by the applied transverse forces will not be encountered. This modeling will unfortunately introduce new problems, namely, the bending moment caused by the longitudinal forces which, according to Eq. 3, should coincide with the centroidal axis. In many cases, though, the effect of axial forces can be neglected.

In order to treat thin-walled open beams in a finite element computer program and include the effects of warping and offset shear center, it will be necessary to either 1) develop a new element that includes these effects, 2) model the beams by a number of plate elements, or 3) arrange the available finite elements in a way consistent with the thin-walled open beam theory. While there exists an element (Ref. 8) with the above features, it is not readily available, and in particular, not for NASTRAN users. A beam modeled by plate elements usually increases the number of grid points tremendously. This also increases the degrees of freedom, and the procedure will often become impractical and uneconomical. One is thus often left to model a thin-walled open beam by the existing beam element which will introduce errors as discussed above or create a new composite element. The following section presents such an element where the effects of warping and offset shear centers are included.

DERIVATION OF A COMPOSITE ELEMENT

Before describing a suitable finite element model, a fictitious continuous beam is presented (Fig. 2). The differential equations of vibration and the corresponding boundary conditions for this beam will be derived by the Hamilton's Variational Principle

$$\delta \int_{t_0}^{t_1} (T - U) dt = 0 \quad (8)$$

where T is the total kinetic and U the total potential energy of the system.

Referring to Fig. 2, the fictitious element consists of a rod coinciding with the centroidal axis, a beam coinciding with the elastic axis, and two flanges displaced h from the elastic axis in a direction parallel to the y coordinate. The rod accepts only axial deformations, and the corresponding strain energy over the whole length, L , of the rod can thus be written as

$$U_R = \frac{1}{2} \int_0^L EA \left(\frac{\partial u}{\partial x} \right)^2 dx \quad (9)$$

where u is the longitudinal displacement of the centroid as defined in the last section.

As indicated in the figure, the beam has all capabilities of a regular beam except that the area is neglected such that no axial strain exists. The strain energy is then given by

$$U_B = \frac{1}{2} \int_0^L \left[EI_1 \left(\frac{\partial^2 v}{\partial x^2} \right)^2 + EI_2^* \left(\frac{\partial^2 w}{\partial x^2} \right)^2 + GJ \left(\frac{\partial \theta}{\partial x} \right)^2 \right] dx \quad (10)$$

in which I_2^* is the moment of inertia about the y -axis while the other properties, including the displacements, are as defined earlier.

The two flanges are displaced from the elastic axis an arbitrary distance h which will be determined later. Only bending deflections are admitted for the flanges, and by defining the displacements parallel to the z -axis as w_1 and w_2 , as indicated on Fig. 2, the strain energy becomes

$$U_F = \frac{1}{2} \int_0^L EI_F \left[\left(\frac{\partial^2 w_1}{\partial x^2} \right)^2 + \left(\frac{\partial^2 w_2}{\partial x^2} \right)^2 \right] dx \quad (11)$$

The rod is assumed to carry all the mass of the elements such that the kinetic energy will be written in terms of the rod displacements u , v^* , w^* , and θ^* . Neglecting rotational inertia, the kinetic energy is

$$T = \frac{1}{2} \int_0^L \rho A \left[\left(\frac{\partial u}{\partial t} \right)^2 + \left(\frac{\partial v^*}{\partial t} \right)^2 + \left(\frac{\partial w^*}{\partial t} \right)^2 + \frac{I_p}{A} \left(\frac{\partial \theta^*}{\partial t} \right)^2 \right] dx \quad (12)$$

where I_p is the centroidal polar moment of inertia and ρ is the mass density of the material.

The nine displacement parameters used will next be reduced to four by the relations

$$\theta^* = \theta \quad (13)$$

$$v^* = v + c_z \theta \quad (14)$$

$$w^* = w - c_y \theta \quad (15)$$

$$w_1 = w + h\theta \quad (16)$$

$$w_2 = w - h\theta \quad (17)$$

c_y and c_z are the distances between C.G. and S.C. in the y and z direction respectively. Substituting these equations into the above expressions for strain and kinetic energies, Hamilton's equation (8) can be formed. The variation is then accomplished by varying u by δu , v by δv , w by δw and θ by $\delta \theta$ where it is understood that the variation vanishes at $t = t_0$ and $t = t_1$. This procedure produces the differential equations

$$EA \frac{\partial^2 u}{\partial x^2} = \rho A \frac{\partial^2 u}{\partial t^2} \quad (18)$$

$$EI_1 \frac{\partial^4 v}{\partial x^4} = -\rho A \frac{\partial^2 v}{\partial t^2} - \rho A c_z \frac{\partial^2 \theta}{\partial t^2} \quad (19)$$

$$E (I_2^* + 2I_F) \frac{\partial^4 w}{\partial x^4} = -\rho A \frac{\partial^2 w}{\partial t^2} + \rho A c_y \frac{\partial^2 \theta}{\partial t^2} \quad (20)$$

$$2EI_F h^2 \frac{\partial^4 \theta}{\partial x^2} - GJ \frac{\partial^2 \theta}{\partial x^2} = -\rho A \left(c_z^2 + c_y^2 + \frac{I_p}{A} \right) \frac{\partial^2 \theta}{\partial t^2} - \rho A c_z \frac{\partial^2 v}{\partial t^2} + \rho A c_y \frac{\partial^2 w}{\partial t^2} \quad (21)$$

and the boundary conditions (at $x = 0$ and $x = 1$)

$$\frac{\partial^2 v}{\partial x^2} \cdot \frac{\partial v}{\partial w} = 0 \quad (22)$$

$$\frac{\partial^3 v}{\partial x^3} \cdot v = 0 \quad (23)$$

$$\frac{\partial^2 w}{\partial x^2} \cdot \frac{\partial w}{\partial x} = 0 \quad (24)$$

$$\frac{\partial^3 w}{\partial x^3} \cdot w = 0 \quad (25)$$

$$\frac{\partial u}{\partial x} \cdot u = 0 \quad (26)$$

$$\frac{\partial^2 \theta}{\partial x^2} \cdot \frac{\partial \theta}{\partial x} = 0 \quad (27)$$

$$\left(2EI_F h^2 \frac{\partial^3 \theta}{\partial x^3} - GJ \frac{\partial \theta}{\partial x} \right) \cdot \theta = 0 \quad (28)$$

The differential equations presented for the thin-walled open beam, Eqs. 3 through 6, can easily be transformed into the form given for the fictitious beam by substituting inertia loads for q_x , q_y , q_z , and m_θ (Ref. 1). Equations 18 through 21 will then become identical with the thin-walled open beam equations if the following two substitutions are made

$$I_2^* = I_2 - 2I_F \quad (29)$$

$$I_F = \frac{C}{2h^2} \cdot \omega \quad (30)$$

It should be observed that the boundary conditions also will be identical with these substitutions.

Because of the mathematical identity between the fictitious and thin-walled open beams, a finite element model for the first will also be a model for the latter. Figure 3 shows how the fictitious beam can be modeled and how the different elements are constrained at the grid points a_0 and b_0 . Four elements will be used; a rod, without torsional rigidity, coinciding with the centroid; a beam, without axial rigidity and mass, coinciding with the elastic axis; and two flanges (or beams), resisting only bending deformations, and displaced h parallel to the y -axis away from the elastic axis. The second

moment of inertia (NASTRAN notation) for the beam and the flanges is as defined in Eqs. 29 and 30, otherwise the notation given in Fig. 3 refers to the original properties of the thin-walled beam. The distance h is arbitrarily chosen, but should be large enough such that I_2^* is positive.

At each grid point, which is arbitrarily taken to be the centroid, the beam is offset by a rigid link to its shear center location. This will insure that the forces acting on the grid points will be transmitted correctly to the beam elements, and the grid point displacements will obey Eqs. 13, 14, and 15 used in the development of the fictitious beam.

Similarly, the displacements of the two flanges must be made dependent upon those at the shear center as restricted by Eqs. 16 and 17. If warping is constrained at the grid point, i.e.,

$$\frac{d\theta}{dx} = 0 \quad (31)$$

then the connections between the flanges and the centroid can be made rigid. Otherwise, as in the case of interior points of a thin-walled open beam, warping is admissible, and Eqs. 16 and 17 imply that

$$\frac{dw_1}{dx} \neq \frac{dw}{dx}, \quad \frac{dw_2}{dx} \neq \frac{dw}{dx} \quad (32)$$

This makes it necessary to create special grid points (a_1 , a_2 , b_1 and b_2 on Fig. 3) for the flanges where the transverse displacements are made dependent displacements, and the rotational displacements

$$\frac{dw_1}{dx} \quad \text{and} \quad \frac{dw_2}{dx}$$

are unrestricted. The four other displacements must, in this case, be constrained in order to avoid singular matrices.

The only difference between the composite model and the fictitious beam is that while Eqs. 16 and 17 are satisfied continuously for the mathematical beam, they are satisfied only at discrete intervals for the model. This implies that the flanges between the grid points will deform according to the law of minimum energy, contributing less to the torsional rigidity than theoretically assumed. Although usually small, this error can be made still smaller by using more grid points along the length of the beam.

NUMERICAL EXAMPLE

A numerical example is presented next to illustrate the use of the composite element and to compare the numerical results with data obtained from theory. The example chosen is the dynamic response of a channel beam whose properties are given by

$$\begin{array}{ll}
A = 0.884 \text{ in}^2 & \rho = 0.733 \cdot 10^{-3} \text{ lbs sec}^2 \text{ in}^{-4} \\
I_1 = 7.66 \text{ in}^4 & C = 3.52 \text{ in}^6 \\
I_2 = 0.294 \text{ in}^4 & c_\omega = 0.0 \text{ in} \\
J = 0.00168 \text{ in}^4 & c^y = 0.94 \text{ in} \\
E = 29 \cdot 10^6 \text{ lbs in}^{-2} & L^z = 120 \text{ in} \\
G = 11 \cdot 10^6 \text{ lbs in}^{-2} &
\end{array}$$

In the pure vibration of the channel beam, the differential equation in the axial displacement u (Eq. 18) uncouples from the other equations. Since c_y is zero in this example, Eq. 20 will uncouple also. The problem then reduces to a coupled vibrational problem in the v - and θ - displacements, Eqs. 19 and 21. For simply supported ends,

$$v = \frac{\partial^2 v}{\partial x^2} = \theta = \frac{\partial^2 \theta}{\partial x^2} = 0 \quad (33)$$

and the theoretical solution, as given by the natural frequencies of vibration, p_i , can be written as (Ref. 3)

$$p_i^2 = \frac{\omega_{ti}^2 + \omega_{bi}^2 \pm \sqrt{(\omega_{ti}^2 - \omega_{bi}^2)^2 + 4\lambda c_z \omega_{bi}^2 \omega_{ti}^2}}{2(1 - \lambda c_z)} \quad (34)$$

where

$$\lambda = \frac{Ac_z}{I_o} \quad (35)$$

$$I_o = I_p + A(c_y^2 + c_z^2) \quad (36)$$

and ω_{ti} and ω_{bi} are the i^{th} uncoupled frequencies in twist and bending, respectively;

$$\omega_{ti}^2 = \frac{GJ\pi^2 L^2 i^2 + EC_\omega \pi^4 i^4}{\rho I_o L} \quad (37)$$

$$\omega_{bi}^2 = \frac{EI_1 \pi^4}{\rho A L^4} i^4 \quad (38)$$

When warping is not included in the analysis, ω_{ti} reduces to

$$\omega_{ti}^2 = \frac{GJ\pi^2L^2i^2}{\rho I_o L^4} \quad (39)$$

The data obtained by using these equations are given in Table 1, cases 1 through 4. It can be observed that warping increases the twisting frequencies more than 100% while an increase of about 5% is seen for the bending frequencies by going from uncoupled to the coupled theory.

The channel is modeled by five equal elements 24 inches in length. Seven different modeling techniques have been tried, and the result is given in Table 1. Cases 5 through 8 show the channel modeled by the conventional Timoshenko beam element coinciding with the centroidal or elastic axis. In the first case only the uncoupled frequencies are obtained, while case 8 reflects the coupled frequencies without taking warping into effect. Also noticeable are the bending frequencies obtained in case 7, which because of the coupling between v and θ , actually represents the twisting frequencies.

Warping is included in the last three cases in Table 1 by using a composite element similar to the one given in Fig. 3, but the rod element is excluded since no axial forces are present during the vibration considered. Because of the boundary conditions, Eq. 33, the flanges must be free to rotate at the ends. This is accomplished by modeling the ends similar to all the interior points with a semi-rigid link where w_1 and w_2 are restricted, but the rotations about the y -axis are free. The bulk data cards used for case 11 are given in the Appendix. Case 9, where the flanges are rigidly linked to the shear center, is included to show how important it is to free the rotational coordinates of the flanges, while cases 10 and 11 show the composite element properly used, including bending displacement and both bending (v) and twisting (θ) displacements, in the numerical analysis. It is noticed that good correlation is obtained between theoretical (case 4) and numerical (case 11) data, the latter results being slightly below the first. This can be reasoned by the fact that few elements are used in the analysis, which implies 1) reduced torsional rigidity as explained above, and 2) concentrated inertia forces at the grid points instead of a continuous distribution.

Although the example did not use the rod element, this must be considered a very special case. For other structures and other loading conditions, the effect of excluding the rod can be significant. This will especially be the case where thin-walled open beams are used as members in between closed beams and where the axial load transfer is large. The example has shown, though, that

- (1) warping effects are properly taken into account by the composite element
- (2) inclusion of rotational displacements are necessary
- (3) good results are obtained with few elements.

CONCLUSION

The composite element presented in this paper has been shown both mathematically and numerically to properly represent the thin-walled open beam. Since it is derived upon the differential equations for such beams, the model can be made as accurate as the theory is. In fact, in the limit as the length of the element gets smaller and smaller, the composite beam element is an exact model of the thin-walled open beam.

In conclusion, it is hoped that future editions of NASTRAN can present a true thin-walled beam element since the need for proper modeling will increase. Until that time, the present composite element is available, it is accurate, and easy to use.

ACKNOWLEDGEMENT

The author expresses his gratitude to Dr. Curtis F. Vail for his many valuable suggestions in carrying out this work.

REFERENCES

1. Vlasov, V. Z., "Thin-Walled Elastic Beams," OTS 61-11400, National Science Foundations, Washington, D.C. (1961).
2. Timoshenko, S. P. and Gere, J. M., Theory of Elastic Stability, Chapter 5, McGraw-Hill, New York, 1961.
3. Timoshenko, S. P., Vibration Problems in Engineering, 3rd Edition, D. Van Nostran Co., Inc., New York, 1955.
4. Gere, J. M., "Torsional Vibration of Beams of Thin-Walled Open Cross Section," Journal of Applied Mechanics, A.S.M.E., December 1954, pp. 381, 387.
5. Gere, J. M. and Lin, Y. K., "Coupled Vibrations of Thin-Walled Beams of Open Cross Section," Journal of Applied Mechanics, Transactions, A.S.M.E., Vol. 80, 1958, p. 373.
6. Christiano, P. and Salmela, L., "Frequencies of Beams with Elastic Warping Restraint," Tech. Note, Journal of the Structural Division, A.S.C.E., Vol. 97, No. ST6, June 1971.
7. Sokolnikoff, I. S., Mathematical Theory of Elasticity, 2nd Edition, McGraw-Hill, New York, 1956.
8. Schrem, E. and Roy, J. R., "An Automatic System for Kinematic Analysis," ASKA Part 1, ISD Report No. 98, Stuttgart, Germany, 1971.

APPENDIX

NASTRAN COMPUTER INPUT DECK

NASTRAN BUFFSIZE=511
 ID SKATTUM,NASTRAN
 APP DISPLACEMENT
 SOL 3,0
 TIME 5
 CEND

TITLE= TEXT BOOK EXAMPLE OF CHANNEL
 METHOD = 13
 MPC = 100

OUTPUT
 DISPLACEMENTS = ALL
 BEGIN BULK

BAR0R							20.	1	
CBAR	1	27	1	2					+CB1
+CB1			0.0	-0.94	0.0	0.0	-0.94	0.0	
CBAR	2	27	2	3					+CB2
+CB2			0.0	-0.94	0.0	0.0	-0.94	0.0	
CBAR	3	27	3	4					+CB3
+CB3			0.0	-0.94	0.0	0.0	-0.94	0.0	
CBAR	4	27	4	5					+CB4
+CB4			0.0	-0.94	0.0	0.0	-0.94	0.0	
CBAR	5	27	5	6					+CB5
+CB5			0.0	-0.94	0.0	0.0	-0.94	0.0	
CBAR	6	2	7	11					
CBAR	7	2	8	15					
CBAR	8	2	14	9					
CBAR	9	2	18	10					
CBAR	12	2	11	12					
CBAR	13	2	12	13					
CBAR	14	2	13	14					
CBAR	22	2	15	16					
CBAR	23	2	16	17					
CBAR	24	2	17	18					
CJNM2	1	1		0.0078					+C21
+C21	0.0767								
CJNM2	2	2		0.0156					+C22
+C22	0.1534								
CJNM2	3	3		0.0156					+C23
+C23	0.1534								
CJNM2	4	4		0.0156					+C24
+C24	0.1534								
CJNM2	5	5		0.0156					+C25
+C25	0.1534								
CJNM2	6	6		0.0078					+C26
+C26	0.0767								
EIGR	13	GIV	0.0	2000.0		10			+13
+13	MAX								
GRID	1		0.0				1234		
GRID	2		24.0						
GRID	3		48.0						
GRID	4		72.0						
GRID	5		96.0						
GRID	6		120.0				1234		
GRID	7		0.0	-0.94	4.0		12345		

GRID	8		0.0	-0.94	-4.0				12345
GRID	9		120.0	-0.94	4.0				12345
GRID	10		120.0	-0.94	-4.0				12345
GRID	11		24.0	-0.94	4.0				1345
GRID	12		48.0	-0.94	4.0				1345
GRID	13		72.0	-0.94	4.0				1345
GRID	14		96.0	-0.94	4.0				1345
GRID	15		24.0	-0.94	-4.0				1345
GRID	16		48.0	-0.94	-4.0				1345
GRID	17		72.0	-0.94	-4.0				1345
GRID	18		96.0	-0.94	-4.0				1345
MAT1	2	29.+6	1.1+7						
MPC	1	11	2	1.0	2	2		-1.0	+MP1
+MP1		2	4	4.0					
MPC	2	12	2	1.0	3	2		-1.0	+MP2
+MP2		3	4	4.0					
MPC	3	13	2	1.0	4	2		-1.0	+MP3
+MP3		4	4	4.0					
MPC	4	14	2	1.0	5	2		-1.0	+MP4
+MP4		5	4	4.0					
MPC	5	15	2	1.0	2	2		-1.0	+MP5
+MP5		2	4	-4.0					
MPC	6	16	2	1.0	3	2		-1.0	+MP6
+MP6		3	4	-4.0					
MPC	7	17	2	1.0	4	2		-1.0	+MP7
+MP7		4	4	-4.0					
MPC	8	18	2	1.0	5	2		-1.0	+MP8
+MP8		5	4	-4.0					
MPCADD	100	1	2	3	4	5	6	7	+MPA
+MPA		8							
OMIT1	5	1	6						
OMIT1	6	7	8	9	10	1	6	18	+OM1
+OM1	17	11	12	13	14	15	16		
OMIT1	1256	2	3	4	5				
PBAR	2	2	0.0	0.0	0.11	0.0			
PBAR	27	2	0.884	7.66	0.074	0.00168			
SEQGP	7	1.2	8	1.4	11	2.2	15	2.4	
SEQGP	12	3.2	16	3.4	13	4.2	17	4.4	
SEQGP	14	5.2	18	5.4					

TABLE 1. FREQUENCIES (CYCLES/SEC.) FOR CHANNEL VIBRATION

Case	Displacement Included	Warping Included	Natural Frequencies					
			Twist			Bending		
			<u>1</u>	<u>2</u>	<u>3</u>	<u>1</u>	<u>2</u>	<u>3</u>
1. Uncoupled theory (Eq. 38)	v	--	--	--	--	63.9	255.5	574.8
2. Uncoupled theory (Eq. 39)	θ	No	7.1	14.2	21.2	--	--	--
3. Uncoupled theory (Eq. 37)	θ	Yes	15.5	56.9	125.8	--	--	--
4. Coupled theory (Eq. 34)	v, θ	Yes	15.4	56.8	125.5	67.1	268.3	603.7
5. Beam along centroidal axis	v	No	--	--	--	63.8	254.4	563.3
6. Beam along centroidal axis	v, θ	No	7.0	13.3	18.2	63.8	254.4	563.3
7. Beam along elastic axis	v	No	--	--	--	7.0	12.9	17.7
8. Beam along elastic axis	v, θ	No	6.7	12.7	17.5	66.6	265.7	588.1
9. Beam along elastic axis	v, θ	Yes*	81.2	134.7	187.3	59.0	269.9	591.0
10. Beam along elastic axis	v	Yes	--	--	--	17.8	63.9	138.5
11. Beam along elastic axis	v, θ	Yes	14.8	54.1	117.7	66.7	266.2	589.1

* Flanges are rigidly linked to the shear center.

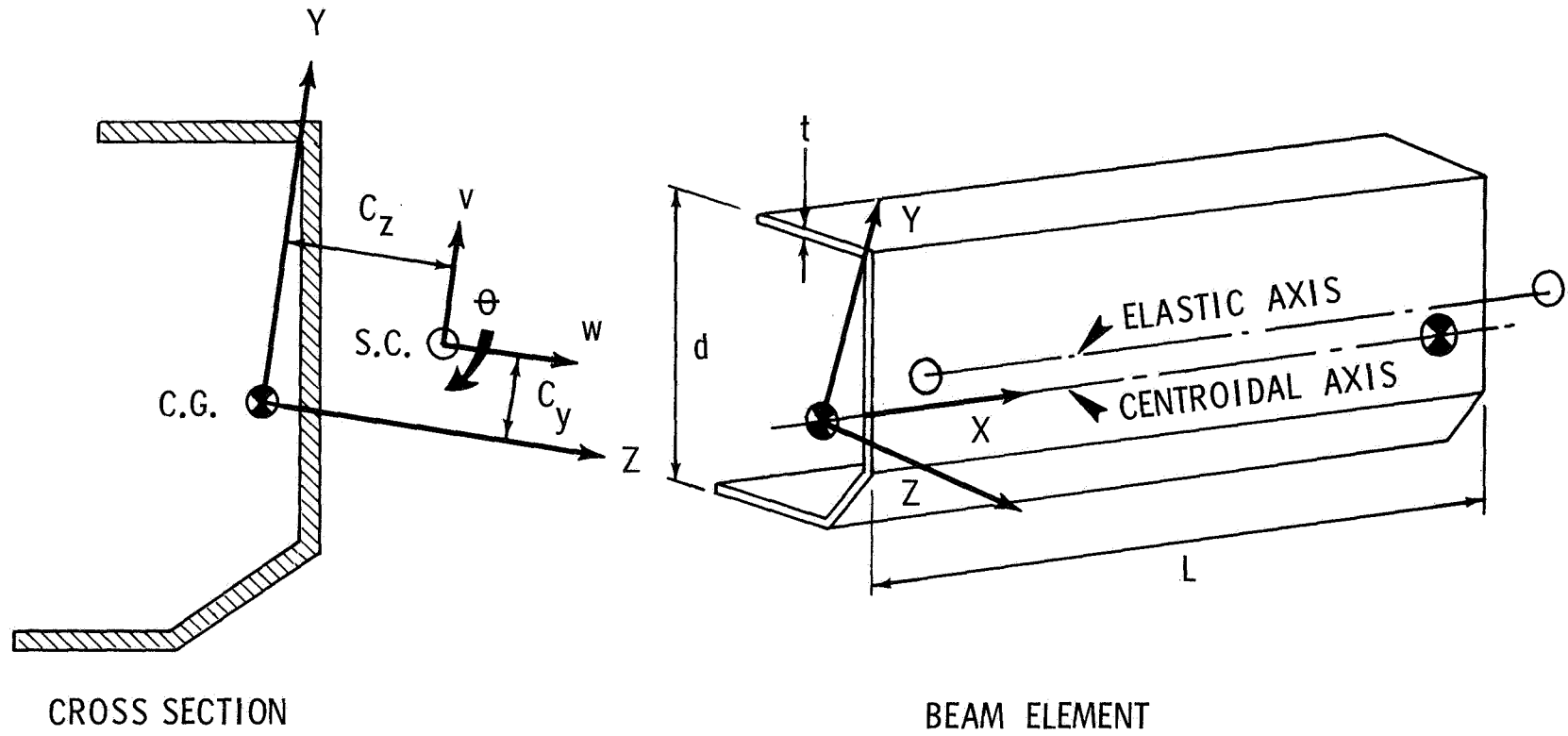


FIG. 1 THIN-WALLED OPEN BEAM

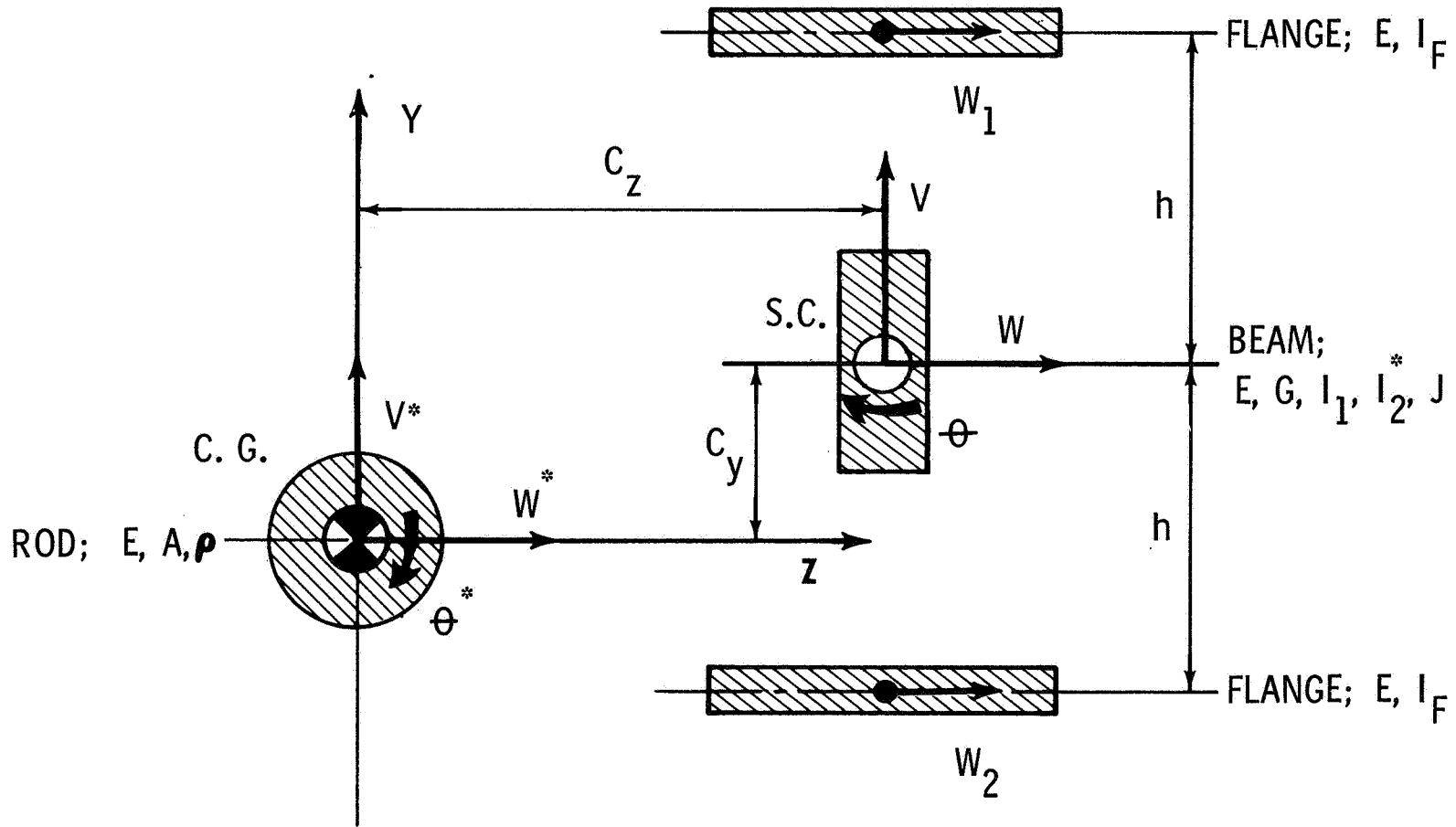


FIG. 2 FICTITIOUS COMPOSITE BEAM

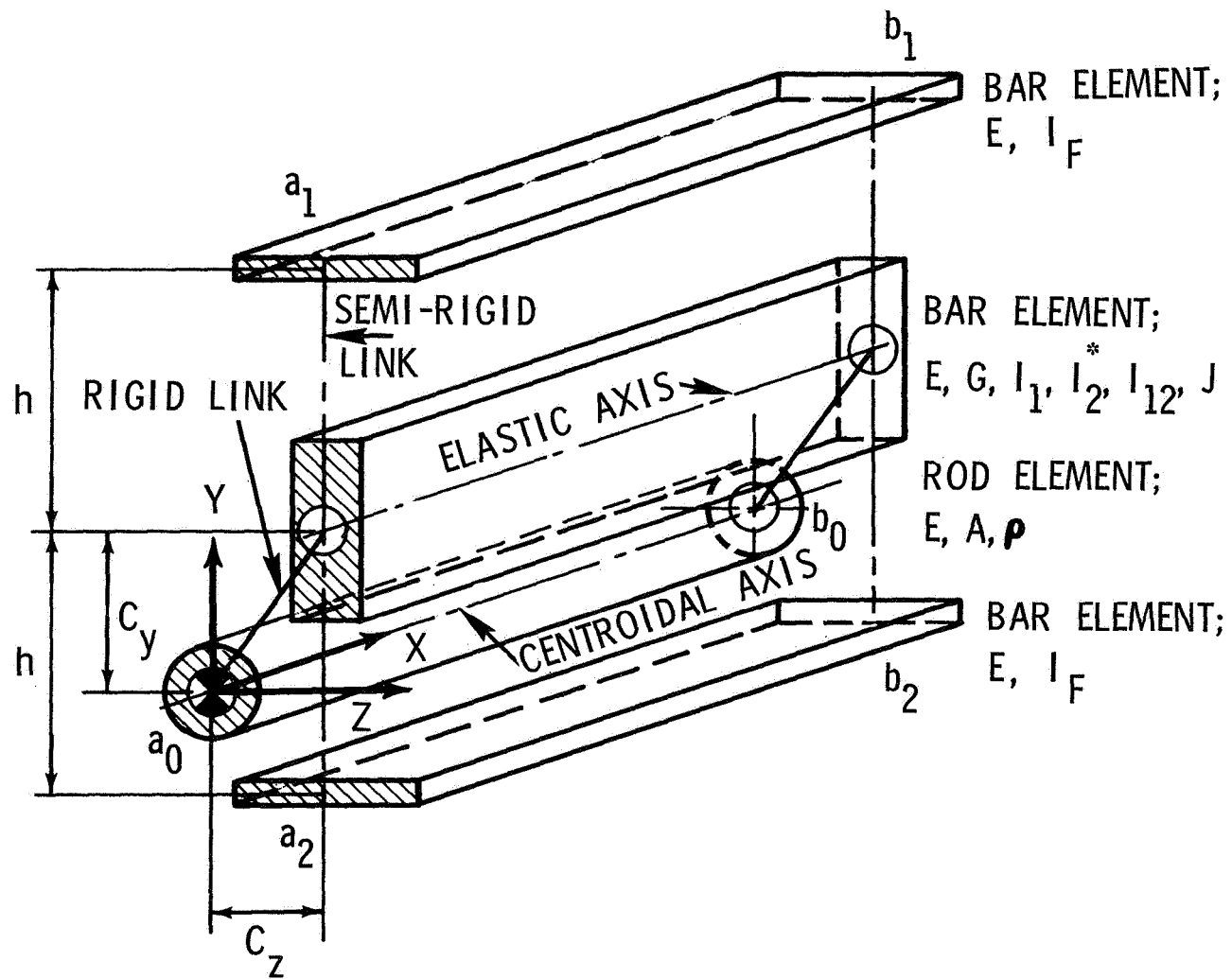


FIG. 3 MODELING OF THIN-WALLED BEAMS OF OPEN CROSS SECTIONS